

Yang Liu 1, Chunna Li 1& Chunlin Gong 1

Shaanxi Aerospace Flight Vehicle Design Key Laboratory, School of Astronautics, Northwestern Polytechnical University, Xi'an 710072, China

#### **Abstract**

During the design, manufacturing, testing and flying of launch vehicles, there are numerous uncertainties of the system and operating environment that affect the design. Uncertain Multidisciplinary Design Optimization (UMDO) is an effective method for evaluating these uncertainties, but it can be challenging to apply it in engineering problems due to high computational costs and slow convergence. To address this issue, we propose a high-fidelity distributed UMDO architecture based on Multiple Discipline Feasibility (MDF). In this architecture, surrogate models are used to quickly evaluate off-line aerodynamic forces and loads instead of conducting aerodynamic discipline analysis. Moreover, we propose to construct uncertainty surrogate models by combining the Maximum Entropy (MaxEnt) for the aerodynamic, engine and structure disciplines to quickly evaluate uncertainties, allowing for efficient solution of the UMDO problems. The proposed UMDO architecture is verified with a liquid launch vehicle optimization problem, and the results demonstrate that the distributed UMDO architecture based on surrogate models can effectively obtain the optimum solution.

**Keywords:** Uncertainty Multidisciplinary Optimization, Uncertainty Quantification, Surrogate model, Launch Vehicle Design

# 1. Introduction

The design, manufacturing and operating of launch vehicle are greatly impacted by many uncertainties stemming from simplified models, material properties and environmental factors, which can lead to system failure[1]. In order to ensure the reliability and safety of the system, uncertainty multidisciplinary design optimization (UMDO) technologies are used to solve the launch vehicle optimization problem under uncertainty[2]. A UMDO process involves multidisciplinary analysis (MDA) to obtain the system response, uncertainty analysis (UA) to acquire system uncertainties, and optimization (OPT) to achieve the optimal design[3]. There are three UMDO architectures based on the loop and the nesting format: the basic architecture OPT-UA-MDA, distributed architecture OPT-MDA-UA, and decoupled architecture OPT-MDA+UA-MDA.

In the basic architecture, MDA is nested within UA as a black-box, of which the state variables are deterministic. This architecture does not introduce additional constraints or errors, but it has the highest computational cost[4]. The decoupled architecture decouples the UMDO as a loop of Multidisciplinary Optimization (MDO) [5] of OPT-MDA and an uncertainty analysis of UA-MDA [6][7]. The uncertainty indicator or standard deviation is propagated between the MDO and UA. Additional constraints are only satisfied in the optimal solution to ensure its feasibility.

In the distributed architecture, the UA is carried out for each discipline, and the uncertainties of state variables are propagated through MDA[8][9]. During uncertainty propagation, the sampling of design and state variables are independent for each discipline. This architecture does not introduce additional constraints, and it shows lower computational cost than the basic architecture[10]. The architecture has more potential in industrial applications because it would not change the existing

design process and specifications. However, since it requires tens of thousands of calls to timeconsuming high-fidelity discipline models in each uncertainty analysis, the UMDO problem cannot be directly solved based on expensive high-fidelity discipline models.

The use of surrogate models is an efficient method to reduce computational cost in solving uncertainty analysis and optimization problem[11][12]. In the distributed UMDO architecture, surrogate models can be used to replace the discipline analysis and discipline uncertainty analysis with parametric inputs and outputs. Such technique is coined surrogate-based UMDO, in which the uncertainty quantification of design and state variables usually adopts a Gaussian distribution or  $3-\sigma$  criterion[13][14]. Hence, accurate uncertainty quantification methods are needed for solving nonlinear problems and problems with high-dimensional state variables such as distributed aerodynamics coefficients.

In order to address the above problem, this paper proposes a unified parametric distributed UMDO architecture based on surrogate models. The MDF is selected as the basic form of the distributed UMDO architecture, whose discipline analysis and discipline uncertainty analysis are approximated by the surrogate models. Then we first use the POD to transform the uncertain high-dimensional data to independent variables, and the statistical moments of those independent parameters, solved by MaxEnt, are used as the unified parameters for quantifying uncertain high-dimensional data. Thus we can build surrogate models with the unified parameters for replacing the discipline analysis and discipline uncertainty analyses. The proposed architecture is validated on a liquid launch vehicle using high-fidelity discipline analysis models, and it demonstrates effective capabilities for solving UMDO problems.

# 2. Proposed Distributed UMDO Architecture

# 2.1 General Form of the Distributed UMDO Architecture

The MDO of the launch vehicle is a loosely-coupled problem. The  $i^{th}$  discipline model of the system can be expressed as  $\mathbf{y}^i = f^i(\mathbf{x}^i, \mathbf{y}^{-i}, \mathbf{d}^i)$ , where  $\mathbf{x}^i$  is a vector of design variables,  $\mathbf{y}^{-i} = [\mathbf{y}^1, ..., \mathbf{y}^{-(i-1)}, \mathbf{y}^{-(i+1)}, ...]$  is a vector of state variables, and  $\mathbf{d}^i$  is a vector of parameters. We use the subscripts D to represent determinacy and U to represent uncertainty, thus the general form of the UMDO problem can be written as:

min 
$$J = f(\mathbf{x}_{D}, \mathbf{x}_{U}, \mathbf{y}_{D}, \mathbf{y}_{U}, \mathbf{d}_{D}, \mathbf{d}_{U})$$
  
w.r.t.  $\mathbf{x}_{D} = [\mathbf{x}_{D}^{1}, ..., \mathbf{x}_{D}^{k}]$   
 $\mathbf{x}_{U} = [\mathbf{y}_{U}^{1}, ..., \mathbf{y}_{U}^{k}]$   
 $\mathbf{y}_{D} = [\mathbf{y}_{D}^{1}, ..., \mathbf{y}_{D}^{k}]$   
 $\mathbf{y}_{U} = [\mathbf{y}_{U}^{1}, ..., \mathbf{y}_{U}^{k}]$   
 $\mathbf{y}^{i} = f^{i}(\mathbf{x}_{D}^{i}, \mathbf{x}_{U}^{i}, \mathbf{y}_{D}^{-i}, \mathbf{y}_{U}^{-i}, \mathbf{d}_{D}^{i}, \mathbf{d}_{U}^{i})$   
s.t.  $\mathbf{g}(\mathbf{x}, \mathbf{y}) \leq 0$ 

where k is the number of disciplines and  $\mathbf{g}$  is the vector of constraints. The general distributed UMDO architecture consists of a three-layer loop consisting of optimization, uncertain multidisciplinary analysis (UMDA), and uncertain disciplinary analysis, as is shown in Figure 1. In terms of the architecture, the distributed UMDO architecture involves uncertainty analysis of the multiple disciplines and uncertainty propagation of the state variables in the MDA. The keys to solve the problem in Equation (1) are the uncertainty quantification and propagation.

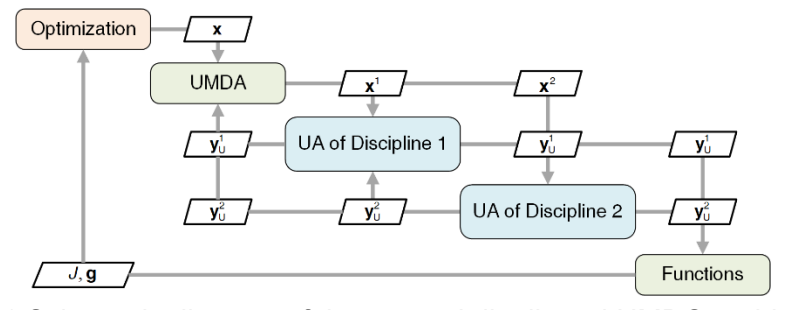


Figure 1 Schematic diagram of the general distributed UMDO architecture.

# 2.2 Parametric Uncertainty Quantification

The parametric uncertainty quantification is used to describe the probability distribution with several parameters. The procedure of the parametric uncertainty quantification is shown in Figure 2. The input of the uncertainty quantification is a sample set  $\bf Z$  of a random variable  $\bf z$ , and the output is a matrix  $\bf \mu$  of quantified parameters. Details of the process are described as follows.

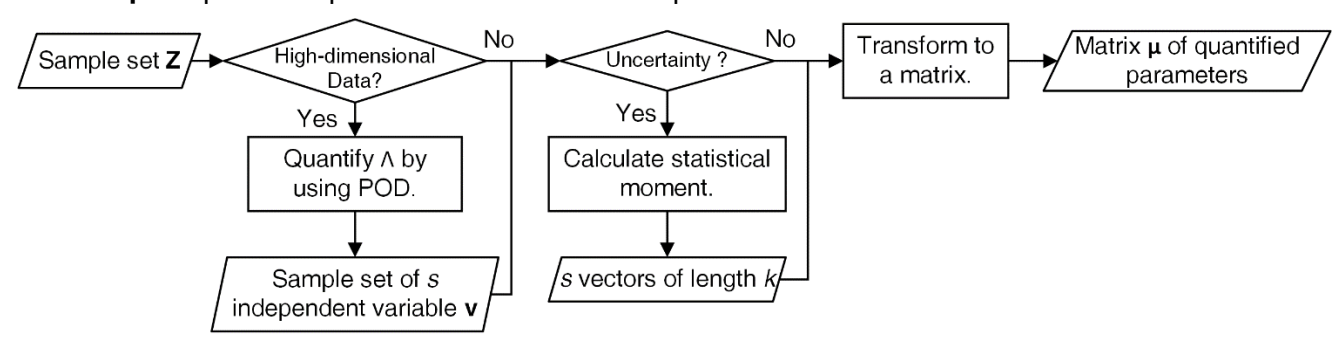


Figure 2 Procedure of the parametric uncertainty quantification.

**Step 1**. If variable  $\mathbf{z}$  is a high-dimensional data, it is necessary to transform  $\mathbf{z}$  to an independent variable vector by Proper Orthogonal Decomposition (POD). Let  $\mathbf{Z} = [\mathbf{z}^1, \mathbf{z}^2, ..., \mathbf{z}^m] \in \mathbb{R}^{n \times m}$  be a sample set of  $\mathbf{z}$ , where m is the number of samples, and n is the number of dimensions. When  $\mathbb{E}(\mathbf{z}) \in \mathbb{R}^n$  is the mathematical expectation of  $\mathbf{z}$ , the covariance matrix  $\mathbf{U}_{cov} \in \mathbb{R}^{n \times n}$  can be obtained by

$$\mathbf{U}_{cov} = (\mathbf{Z} - \overline{\mathbf{z}})(\mathbf{Z} - \overline{\mathbf{z}})^{\mathsf{T}}$$

$$\overline{\mathbf{z}} = \left[ \mathbb{E}(\mathbf{z}), \mathbb{E}(\mathbf{z}), ..., \mathbb{E}(\mathbf{z}) \right] \in \mathbb{R}^{n \times m}$$
(2)

By solving the characteristic equations of the covariance matrix, we can obtain the eigenvalue vector  $\chi = [\chi_1, \chi_2, ..., \chi_n]^{\mathsf{T}}$  and  $\Xi = [\xi_1, \xi_2, ..., \xi_n] \in \mathbb{R}^{n \times n}$  of  $\mathbf{U}_{cov}$ . Then  $\chi_i (i = 1, ..., n)$  are sorted in a descending order, and  $\xi_i (i = 1, ..., n)$  are sorted accordingly. The truncated order s, which is also the dimension of the parameters after reduction, is selected by energy proportion  $c_e$ :

$$C_{e} = \sum_{j=1}^{s} \frac{\chi_{j}}{\|\mathbf{x}\|_{1}} > \varepsilon \tag{3}$$

where  $\varepsilon \in [0.95, 0.9999]$ . The *s* eigenvectors form the mode matrix  $\mathbf{U}_{m} = [\boldsymbol{\xi}_{1}, \boldsymbol{\xi}_{2}, ..., \boldsymbol{\xi}_{s}] \in \mathbb{R}^{n \times s}$ . Then the according model coefficients matrix  $\mathbf{V}$  can be obtained by

$$\mathbf{v}_{i} = \mathbf{U}_{m}^{\mathsf{T}} \mathbf{z}_{i} \in \mathbb{R}^{s} \qquad i = 1, 2, ..., m$$

$$\mathbf{V} = \begin{bmatrix} \mathbf{v}^{1}, \mathbf{v}^{2}, ..., \mathbf{v}^{m} \end{bmatrix} \in \mathbb{R}^{s \times m}$$
(4)

The *n*-dimensional high-dimensional data  $\mathbf{z}$  can be expressed by a *s*-dimensional independent uncertain vector  $\mathbf{v}$  with the sample set  $\mathbf{V}$ . If  $\mathbf{z}$  is numerical value,  $\mathbf{v}$  can be obtained by  $\mathbf{v} = \mathbf{z} \in \mathbb{R}^{n \times 1}$ .

**Step 2**. If **v** is an uncertain vector, the statistical moments of **v** are computed as the quantified parameters. Let  $\mu = \mathbb{E}(\mathbf{v})$  be the mathematical expectation of **v**, the  $k^{\text{th}}$  central moment  $\mu_k$  (k = 2, 3, ...) can be obtained by sample set **V**:

$$\mu_{k} = \frac{1}{m} \sum_{i=1}^{m} \left( v^{i} - \mu \right)^{k} \tag{5}$$

Then the vector of the moments is  $\boldsymbol{\mu} = \left[\mu, \mu_2, ... \mu_k\right] \in \mathbb{R}^k$ . Since  $\boldsymbol{v}$  consists of  $\boldsymbol{s}$ -independent variables,  $\boldsymbol{\mu}_1$  to  $\boldsymbol{\mu}_s$  are computed independently.

**Step 3**. Form the parameters matrix  $\boldsymbol{\mu} = [\boldsymbol{\mu}_1, ..., \boldsymbol{\mu}_s]^T \in \mathbb{R}^{s \times k}$ , which is detailed as:

$$\mathbf{\mu} = \begin{bmatrix} \mu_{1} & \mu_{1,2} & \dots & \mu_{1,k} \\ \mu_{2} & \mu_{2,2} & \dots & \mu_{2,k} \\ \dots & \dots & \dots & \dots \\ \mu_{s} & \mu_{s,2} & \dots & \mu_{s,k} \end{bmatrix}$$
 (6)

The 1<sup>st</sup> column represents the expectation vector  $\mathbb{E}(\mathbf{v})$ , and the others represent the moments. If  $\mathbf{z}$  is a deterministic value, s=k=1, and  $\mathbf{\mu}=[\mu_1]$ . If  $\mathbf{z}$  is an uncertain value, s=1, k>1, and  $\mathbf{\mu}=[\mu_1,\mu_{1,2},...\mu_{1,k}]$ . If  $\mathbf{z}$  is a deterministic high-dimensional data, s>1, k=1, and  $\mathbf{\mu}=[\mu_1,\mu_2,...\mu_s]^T$ . If  $\mathbf{z}$  is an uncertain high-dimensional data, s>1, k>1.

By the above way, a set of samples of the state variables can be parameterized as  $\mu$ . Then the inverse parameterization for obtaining a set of samples under the given  $\mu$  is shown in Figure 3. The inverse parameterization procedure also consists of three steps.

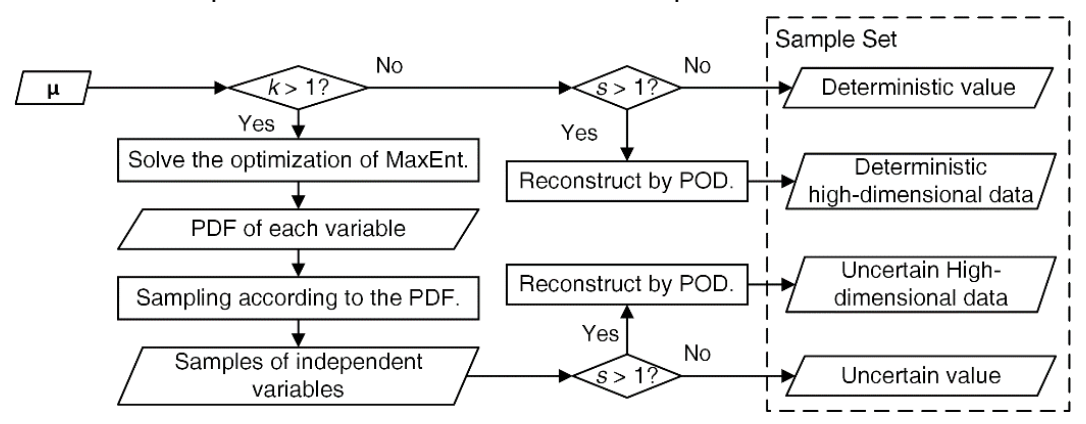


Figure 3 Procedure of the inverse parameterization.

**Step 1**. If k > 1,  $\mu$  represents an uncertain variable. For each row of  $\mu$ , the probability density function (PDF) p(x) is calculated via Maximum Entropy that builds an analytical function of:

$$\rho(x) = e^{\sum_{i=0}^{n} \lambda_i (x-\mu)^i}$$
 (7)

where  $\lambda_i$  (i=0,...,k) are the coefficients of the Lagrange Multiplier Method. Then  $\mathbf{\lambda} = \begin{bmatrix} \lambda_1,...\lambda_k \end{bmatrix}^T$  can be obtained by solving an optimization problem:

given 
$$\mu$$
  
min  $J = \sum_{i=1}^{k} r_i^2$   
w.r.t.  $\mathbf{\lambda} = \begin{bmatrix} \lambda_1, ... \lambda_k \end{bmatrix}^T$   
where  $r_i = \int_{-\infty}^{+\infty} (x - \mu)^i p(x, \mathbf{\lambda}) dx - \mu_i$  (8)

The Differential Evolution (DE) is used to search for suitable initial values of  $\lambda$ , and then the SD algorithm is used to solve the above optimization problem in Equation(8). Then with the optimal coefficients, the p(x) can be computed by Equation (7). If k = 1, go directly to step 3.

**Step 2**. Generate a set of *s*-dimensional *q* samples  $\mathbf{V} \in \mathbb{R}^{s \times q}$  according to obtained PDFs. Then if s > 1, the sample set of the uncertain high-dimensional data  $\mathbf{Z} \in \mathbb{R}^{n \times q}$  can be calculated by:

$$\mathbf{Z} = \mathbf{U}_{\mathbf{m}} \mathbf{V} + \mathbb{E}(\mathbf{z}) \tag{9}$$

If s = 1, the sample set of the uncertain value is  $\mathbf{Z} = \mathbf{V} \in \mathbb{R}^{1 \times q}$ .

**Step 3**. If k=1 and s=1,  $\mu$  represents a deterministic value  $\mathbf{Z}=\mu_1\in\mathbb{R}^{1\times 1}$ . If k=1 and s>1,  $\mu$  represents the expectation of the s modes  $\mathbf{V}=\mu^T\in\mathbb{R}^{s\times 1}$ . Then the deterministic numerical value  $\mathbf{Z}\in\mathbb{R}^{n\times 1}$  can be obtained by Equation (9).

# 2.3 Distributed UMDO Architecture Based on Surrogate models

Using the parametric uncertainty quantification method,  $\mathbf{x}_{\text{D}}$ ,  $\mathbf{x}_{\text{U}}$ ,  $\mathbf{y}_{\text{D}}$ ,  $\mathbf{y}_{\text{U}}$ ,  $\mathbf{d}_{\text{C}}$  and  $\mathbf{d}_{\text{U}}$  can be all quantified by  $\boldsymbol{\mu}$ . For ease of differentiation, we use notation  $[\tilde{\mathbf{x}}, \tilde{\mathbf{y}}, \tilde{\mathbf{d}}]$  to replace  $\boldsymbol{\mu}$ . Since high-fidelity discipline analyses cannot be directly employed in the UMDO solution process due to expensive computational cost, surrogate models are usually used to approximate the discipline analyses and the uncertainty propagation. The above two kinds of surrogates are used as black-box models, and they can be uniformly expressed as:

$$\begin{cases} \hat{\mathbf{y}}^{i} = \hat{\mathbf{f}} \left( \tilde{\mathbf{x}}^{i}, \tilde{\mathbf{y}}^{-i} \right) \\ \left\| \tilde{\mathbf{y}}^{i} - \hat{\mathbf{y}}^{i} \right\| \leq \varepsilon \end{cases}$$
 (10)

where  $\hat{\mathbf{y}}$  is predicted  $\tilde{\mathbf{y}}$ ,  $\boldsymbol{\varepsilon}$  is allowed error of prediction. We use a two-layer nested analysis to build surrogate models, as is shown in Figure 4. The outer-layer is to generate the mathematic expression of  $\tilde{\mathbf{x}}^i$ ,  $\tilde{\mathbf{y}}^{-i}$  within the design space. If  $\tilde{\mathbf{x}}^i$ ,  $\tilde{\mathbf{y}}^{-i}$  and  $\tilde{\mathbf{d}}^i$  are uncertain, the inner-layer is uncertainty analysis of each  $\mathbb{E}(\tilde{\mathbf{x}})$ . If they are deterministic, the inner-layer is discipline analysis. Then parametric uncertainty quantification is carried out to obtain  $\tilde{\mathbf{y}}^i$ . Then the surrogate models  $\hat{\mathbf{y}}^i = \hat{\mathbf{f}}(\tilde{\mathbf{x}}^i, \tilde{\mathbf{y}}^{-i})$  is trained based on the input  $[\tilde{\mathbf{x}}^i, \tilde{\mathbf{y}}^{-i}]$  and output  $\tilde{\mathbf{y}}^i$ .

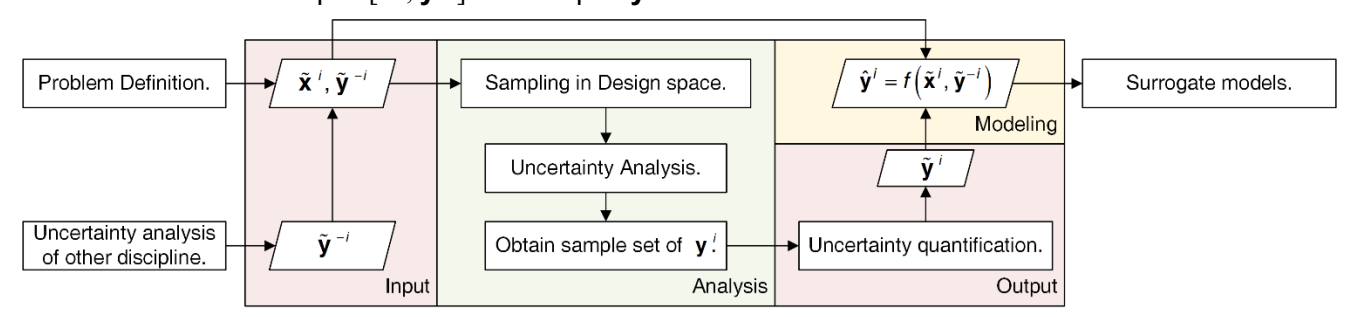


Figure 4 Surrogate modeling process.

The surrogate models for uncertainty propagation must be built sequentially, as the design space is determined by the previous discipline analysis. Besides, the surrogate modeling process should be offline to taking advantage of high-fidelity analyses by high performance computations in parallel. We apply the proposed parametric uncertainty quantification and surrogate modelling methods in the distributed UMDO, and the mathematical expression of the UMDO problem can be expressed as:

min 
$$J = f(\tilde{\mathbf{x}}, \hat{\mathbf{y}}, \tilde{\mathbf{d}})$$
  
w.r.t.  $\tilde{\mathbf{x}}$   
 $\hat{\mathbf{y}}^i = f_i(\tilde{\mathbf{x}}^i, \tilde{\mathbf{y}}^{-i}, \tilde{\mathbf{d}})$   
s.t.  $\mathbf{g}(\mathbf{x}, \mathbf{y}) \le 0$  (11)

Since all the elements of  $[\tilde{\mathbf{x}}, \tilde{\mathbf{y}}, \tilde{\mathbf{d}}]$  are independent, the distributed UMDO problem has the same mathematical representation as the MDO problem. Therefore, the general MDO architectures can still be used in the distributed UMDO architecture, such as Individual Discipline Feasible (IDF), MDF, BLISS-2000. For an engineering optimization problem, improving the feasibility and convergence of the optimization problem is the primary issue. Therefore, we recommend the MDF-class architecture to solve the problem in Equation(11).

# 3. Study Case of a Launch Vehicle Optimization

## 3.1 Discipline models of the Launch Vehicle

The studied launch vehicle is a one-and-a half-stage rocket with four boosters. Both the core stage and the booster use 2 identical liquid engines, whose propellants are liquid oxygen (LOX) and methane (CH4). The task of the launch vehicle is to deliver a 50,000 kg load to an orbit with a half-length axis of 6,629,387 m, an eccentricity of 0.012104, and an orbital inclination of 0.723962 rad. The diameters of the core stage and the boosters are respectively 5m and 3.35m. Each booster has a fixed wing with a fixed size.

The disciplines of the launch vehicle involve aerodynamics, engine, structure, mass, trajectory and guidance and control. Computational Fuild Dynamics (CFD) is used as the discipline analysis model in the aerodynamics discipline, which is used to calculate the drag coefficients  $C_{\rm D}$ , lift coefficients  $C_{\rm L}$ , and distributed pressure coefficient  $C_{\rm P}$  for different aerodynamic shapes and flight conditions. The parameters of the aerodynamic shape are the lengths of the core stage and boosters, whose variation ranges are shown in Figure 7.

The analysis model of the engine is CEA, which computes the specific impulse  $I_{\rm S}$  based on oxygen-fuel ratio  $r_{\rm P}$ , expansion ratio of the nozzle  $r_{\rm N}$ , and pressure of the combustor  $p_{\rm C}$ . Then the thrust can be obtained by  $F_{\rm P} = I_{\rm S} \cdot r_{\rm E} \cdot \dot{m}_{\rm P}$ , where  $r_{\rm E}$  is efficiency of the nozzle, and  $\dot{m}_{\rm P}$  is total mass flow of the LOX and CH4. The parameters of the 10 identical engines are the same in the analysis model, but the uncertainty is calculated independently for each engine.

The structure discipline is built to calculate the structure mass  $m_{\rm S}$  under the given loads while ensuing the structural reliability. The loads include aerodynamic load  $C_{\rm P}$ , axial and normal forces of engine  $F_{\rm P}$ . The structural reliability for the  $i^{\rm th}$  component is  $\mathbb{P}(\sigma_i < \sigma_i^*)$ , where  $\sigma_i$  is the maximum stress of the  $i^{\rm th}$  component, and  $\sigma_i^*$  is allowed yield strength of the  $i^{\rm th}$  component. Then the total reliability can be expressed as:

$$\mathbb{P}_{S}(\boldsymbol{\sigma}_{S} < \boldsymbol{\sigma}^{*}) = \prod_{i=1}^{N} \mathbb{P}(\boldsymbol{\sigma}_{i} < \boldsymbol{\sigma}_{i}^{*})$$
(12)

where N is the number of components. The maximum stress is computed by the Finite Element Method (FEM), which was carried out individually for each component in bottom-to-top order. The loads at the interfaces of different components are calculated by interpolation to ensure the accuracy. The lengths and diameters of the components are fixed parameters, and the thicknesses  $\mathbf{t}_{\mathrm{S}}$  of the tanks, fairing and interstages are design variables. Structure mass  $m_{\mathrm{S}}$  is obtained by solving an optimization problem:

min 
$$m_{\rm S}$$
  
w.r.t.  $\mathbf{t}_{\rm S}$  (13)  
s.t.  $\mathbb{P}_{\rm S}(\boldsymbol{\sigma}_{\rm S} < \boldsymbol{\sigma}^*) \ge 0.999$ 

The mass discipline calculates the propellant mass  $m_{\rm P}$ , total mass  $m_{\rm T}$ , and centroid  $X_{\rm C}$ . The liquid propellant height are design variables. The length of the tank is calculated based on the liquid propellant height, and the ellipsoidal ratios of the tanks are fixed parameters.

The trajectory discipline plans a standard trajectory with deterministic inputs. Then the guidance and control disciplines track the standard trajectory and the orbit with uncertain inputs. The three-degree kinetic equations are used as the trajectory model, then a pseudo-spectral approach with the objective of minimizing the remaining propellant mass  $m_{\rm R}$  is employed to optimize the trajectory. For the guidance discipline, the perturbation guidance is applied before separation of boosters to track the standard trajectory, and iterative guidance is used after the separation to track the orbit. Finally, PID is applied as control model to calculate the angle of nozzle. The reliability of the mission  $P_{\rm M}$  is the probability of successful orbit, where the failure of the mission n happens when the launch vehicle cannot satisfy the parameters of the orbit after consuming all the propellant.

# 3.2 Definition of the Launch Vehicle UMDO Problem

The design space and uncertainties of the variables and parameters are defined in Table 1.

 $N(\mu,\sigma)$  represents Gaussian distribution, and  $U(\mu,a)$  represents uniform distribution, where a is the half length of the interval. The surrogate models for replacing the aerodynamic and engine discipline analyses, as well as the structure discipline uncertainty analysis, are built within the design space. Surrogate models for  $C_D$  and  $C_L$  are built with the inputs of the lengths of the core stage and boosters, the Mach number Ma and the angle of attack  $\alpha$ . The distributed aerodynamic loads  $C_P$  are modeled with BPNN combined with POD. The maximum errors of  $C_D$  and  $C_L$  are both less than 5%, and the maximum error of  $C_P$  is less than 3%. For structure discipline, the uncertainties of maximum stress  $\sigma_i$  of each component are also modeled by Back Propagation Neural Network (BPNN) combined with POD. The average prediction error of the LOX tank is 0.89%, and the error of the predicted variance is 2.45%.  $I_S$  is modeled by Kriging, and the maximum error of the expectation is 0.03%, while the error of the variance is 1.15%.

Table 1 Design space and uncertainties of the variables and parameters.

Parameters	Notation	Units	Design Space	Uncertainty
Mass flow of CH4	$\dot{m}_{\scriptscriptstyle P,CH4}$	kg/s	[120,150]	$N(\sim,2)$
Mass flow of LOX	$\dot{m}_{\scriptscriptstyle P,LOX}$	kg/s	[573, 700]	$N(\sim,5)$
CH4 level height of the Core	$h_{\scriptscriptstyle C,CH4}$	m	[13,18]	$U(\sim, 0.1)$
LOX level height of the Core	$h_{\scriptscriptstyle C,LOX}$	m	[18, 24]	$U(\sim, 0.1)$
CH4 level height of Boosters	$h_{\scriptscriptstyle B,CH4}$	m	[11.5,14.5]	$U(\sim, 0.1)$
LOX level height of Boosters	$h_{\scriptscriptstyle B,LOX}$	m	[16, 21]	$U(\sim, 0.1)$
Pitch angle	$\varphi$	0	[-90, 90]	-
Sideslip angle	Ψ	0	[-30, 30]	-
Thicknesses of the structure	t <sub>s</sub>	m	[0.005, 0.012]	-
Drag coefficients	$C_{D}$	-	-	U(~,10%)
Lift coefficients	$C_{L}$	-	-	U(~,10%)
Distributed pressure coefficients	$C_P$	-	-	U(~,10%)
Atmospheric density	$ ho_{\scriptscriptstyleA}$	$kg/m^3$	-	$U(\sim,3\%)$
Atmospheric pressure	$p_A$	Pa	-	$U(\sim,5\%)$
Gravity	g	$m/s^2$	-	U(~,1%)
Expansion ratio of the nozzle	$r_{_{ m N}}$	-	-	N(35, 0.1)
Efficiency of the nozzle	$r_{\scriptscriptstyle \sf E}$	-	-	N(0.95, 0.002)
Pressure of combustor	<b>p</b> <sub>C</sub>	MPa	-	N(10.2, 0.15)
Angle of attack and sideslip	α, β	0	-	$U(\sim,0.2)$
Structure Mass	m <sub>s</sub>	kg	-	$N(\sim, 0.2\%)$

Since the analysis model of the mass discipline is analytical, we use Monte Carlo Simulation (MCS) for uncertainty analysis of the mass discipline. The uncertainty analysis of guidance combined with control requires a very high accuracy, which is difficult to achieve with surrogate models. Therefore, we also use MCS for uncertainty analysis of the guidance discipline, which takes more than 70% of simulation time of MDA.

The optimization problem involves three optimization problems: system optimization, trajectory

optimization, and structure optimization. The mathematical expressions of the problems are expressed as follows:

System Optimization

min 
$$m_{\text{T}}$$
  
w.r.t.  $\mathbf{x} = [\dot{m}_{\text{P}}, r_{\text{P}}, h_{\text{C,CH4}}, h_{\text{C,LOX}}, h_{\text{B,CH4}}, h_{\text{B,LOX}}]$   
s.t.  $\mathbf{x} \in [\mathbf{x}_{\text{min}}, \mathbf{x}_{\text{max}}]$   
 $\mathcal{P}_{\text{M}} \ge 0.99$ 

**Trajectory Optimization** 

min 
$$-m_R$$
  
w.r.t.  $\mathbf{x} = [\varphi, \psi]$   
s.t.  $\mathbf{x} \in [\mathbf{x}_{min}, \mathbf{x}_{max}]$   
 $\varepsilon_{Orbit} \le 10^{-6}$  (14)

Structure Optimization

min 
$$m_s$$
  
w.r.t.  $\mathbf{x} = [\mathbf{t}_s]$   
s.t.  $\mathcal{P}_s(\mathbf{\sigma}_s < \mathbf{\sigma}^*) \ge 0.999$ 

where  $\varepsilon_{\text{Orbit}}$  is the relative error of the orbiting. The system optimization is solved by the DE algorithm. The size of the population is set to 120, and the maximum iteration steps is set to 100. The optimization is run in parallel using 5 cores. The trajectory optimization is solved by the Sparse Nonlinear Optimizer algorithm, and the structure optimization is solved by the Sequence Quadratic Programming algorithm. The design structural matrix of the optimization problem is represented in Figure 5, where q is the dynamic pressure, and h is the current liquid propellent height.

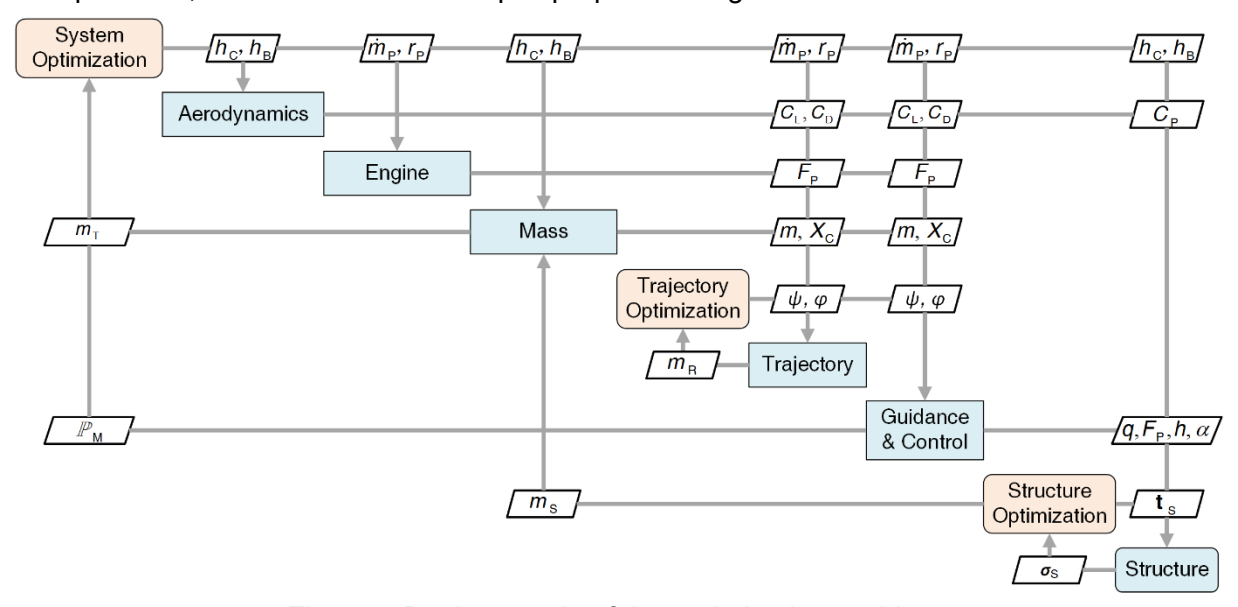


Figure 5 Design matrix of the optimization problem.

# 3.3 Results Analysis

After optimization, UMDA is called 12000 times, and the simulation time is 119.3 hours. The convergence history of the objective function and the reliability constraint are shown in Figure 6. In the Figure 6, the objective function is normalized with the penalty of the reliability constraint. At the beginning of the optimization, the objective function is very large due to the violation of  $\mathbb{P}_{\rm M}$ . The constraint is fully satisfied after the 19<sup>th</sup> iterations, then the direction of the optimization is to reduce  $m_{\rm T}$ . From the 19<sup>th</sup> to the 100<sup>th</sup> iteration,  $m_{\rm T}$  is reduced by 98,379 kg.

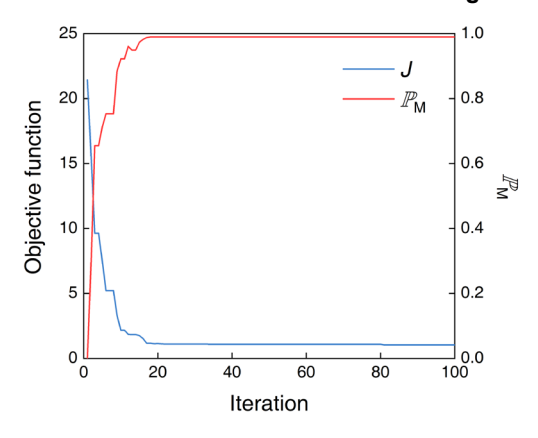


Figure 6 Iteration of the system optimization.

The important optimal design variables, state variables and response are presented in Table 2. The payload-weight ratio of the launch vehicle is 0.0285, and the launch thrust-weight ratio is 1.277. To obtain a larger launch thrust, the  $\dot{m}_{\rm P}$  approaches the upper bounds. Since the engine shuts down when either LOX or CH4 is consumed, the ratio of propellant mass of LOX and CH4 is close to  $r_{\rm P}$ . The optimum shape is middle of the allowed size range, as is shown in Figure 7.

Table 2 Optimal solution.

Parameters	Value	Units	Variables	Value	Units
$m_{\scriptscriptstyle  extsf{T}}$	1759706	kg	$\dot{m}_{_{\mathrm{P}}}$	694.27	kg/s
$m_{\rm s}$	144234	kg	$r_{_{\mathrm{P}}}$	2.6618	-
$m_{\scriptscriptstyleR}$	6758	kg	$h_{\scriptscriptstyle C,CH4}$	15.435	m
${\mathbb P}_{\mathsf M}$	0.9903	-	$h_{\scriptscriptstyle C,LOX}$	20.986	m
F <sub>P</sub> (Vacuum)	2387.5	kN	$h_{\scriptscriptstyle B,CH4}$	14.279	m
I <sub>s</sub> (Vacuum)	350.83	s	$h_{\scriptscriptstyle B,LOX}$	19.545	m

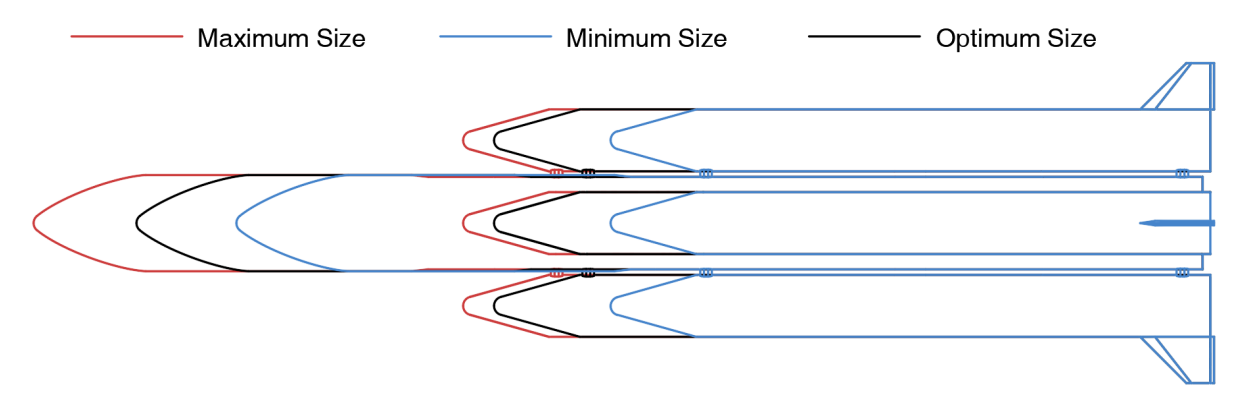
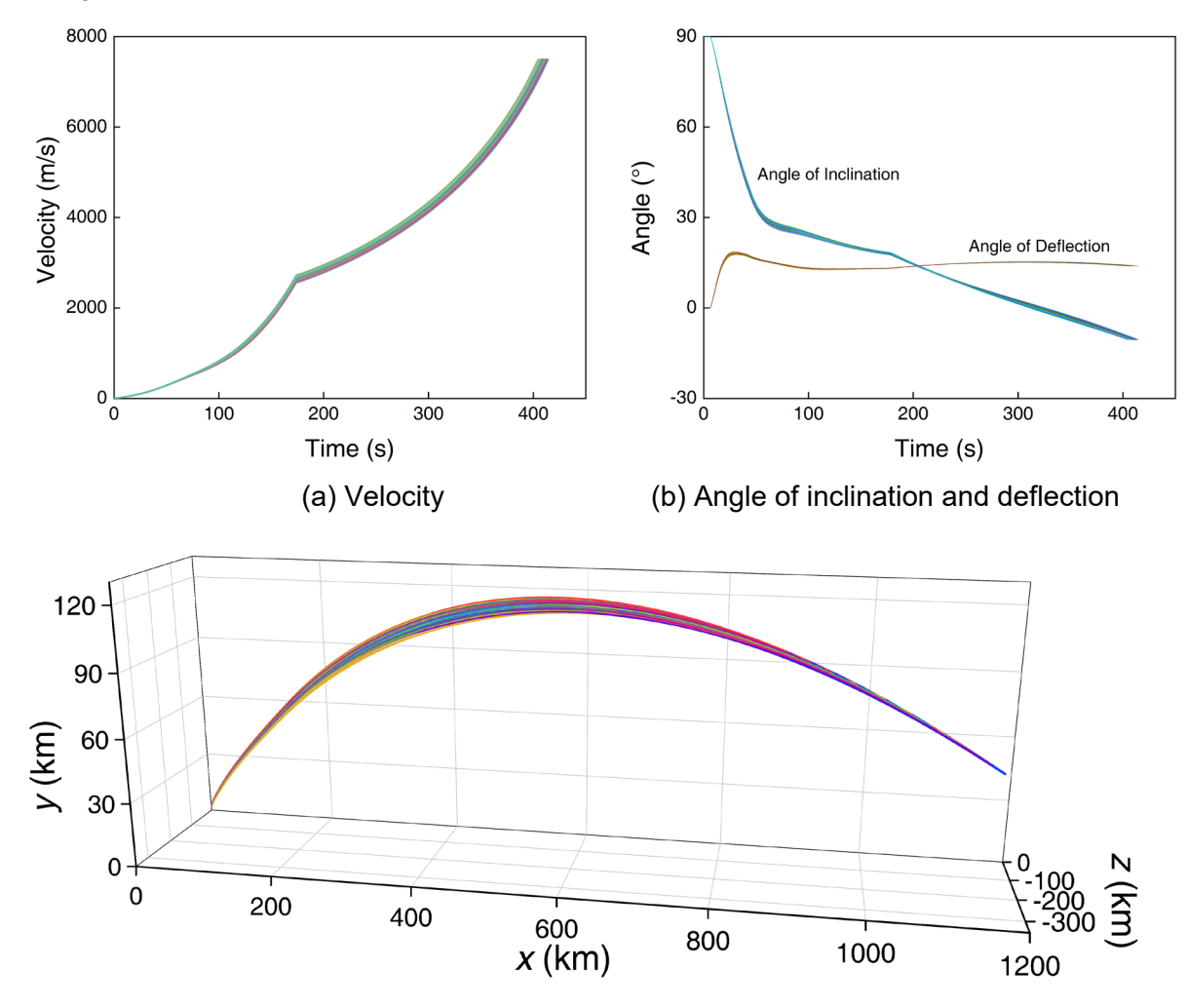


Figure 7 Maximum, minimum and optimum size of the launch vehicle.

The uncertainties of parameters along the trajectory are shown in Figure 8. At the time of 173.7 s after launching, the booster separates at the height of 60 km. The uncertainty in velocity is compensated by increasing the flight time to eventually reach the point of orbiting. Therefore, in order to satisfy the constraint of  $\mathbb{P}_{\rm M}$ , 6758 kg of  $m_{\rm R}$  is needed. The uncertainty of the angle of inclination is greater than that of angle of deflection because there are more uncertainties in vertical direction,

including gravity, atmospheric pressure and altitude. According to Figure 8(c), the deviation of the rocket is the largest at the highest point of the trajectory, and then it gradually decreases due to the iterative guidance.



(c) Trajectory in Launch coordinate system.

Figure 8 Uncertainties of the trajectory.

The uncertainty distributions of the oxygen-fuel ratio  $r_{\rm P}$ , specific impulse  $I_{\rm S}$ , separation time of the booster, terminal time of the core, total mass flow  $\dot{m}_{\rm P}$  and vacuum thrust  $F_{\rm P}$  are respectively shown in Figure 9. The PDFs are acquired by quantifying the uncertainties based on 10,000 samples. All the 6 PDFs are not Gaussian. The PDF shapes of  $r_{\rm P}$ ,  $F_{\rm P}$  and  $\dot{m}_{\rm P}$  are close to trapezoidal distributions. The skewness of  $I_{\rm S}$  is only 0.016, but the shape of PDF is not symmetrical. The separation time of the booster completely depends on the propellant mass and  $\dot{m}_{\rm P}$ , while the terminal time of the core depends on the guidance.

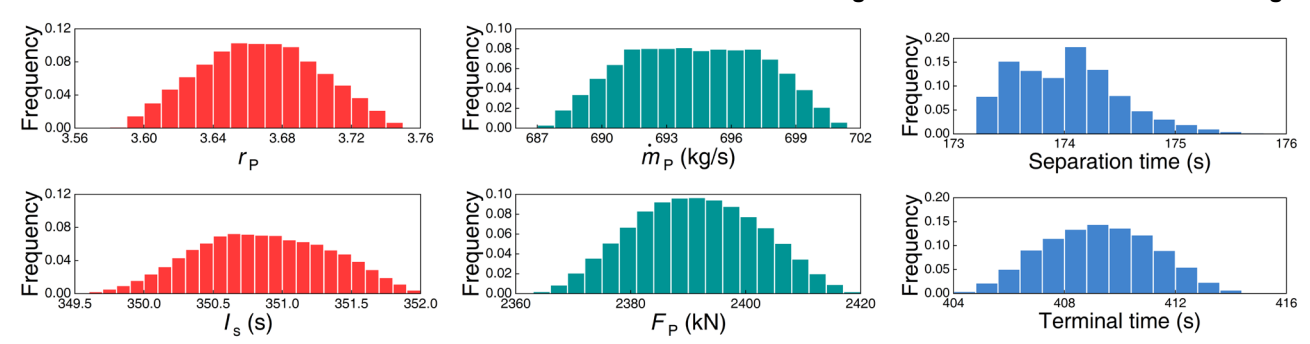


Figure 9 Distribution of important parameters.

#### 4. Conclusion

To reduce the expensive computational cost by solving the UMDO problem with high-fidelity discipline analyses, a parametric distributed UMDO architecture based on surrogate models is proposed. We use POD to transform the high-dimensional data to independent parameters, then calculate the statistical moments to parameterize the uncertainty of the parameters. The MaxEnt is used to obtain the PDF by solving an optimization problem with quantified parameters. Moreover, the surrogate-based uncertainty propagation method is developed to approximate the discipline uncertainty analysis in the UMDO architecture. Thus, the UMDO problem can be converted to a MDO problem, which can be effectively solved by mature MDO architecture. The proposed architecture is verified with a liquid launch vehicle optimization problem, and the results indicate that the proposed architecture can effectively obtain the optimal solution.

# 5. Acknowledgement

This work is funded by the major advanced research project of Civil Aerospace from State Administration of Science Technology and Industry of China.

#### 6. Contact Author Email Address

Mailto: chunnali@nwpu.edu.cn

# 7. Copyright Statement

The authors confirm that they, and/or their company or organization, hold copyright on all of the original material included in this paper. The authors also confirm that they have obtained permission, from the copyright holder of any third party material included in this paper, to publish it as part of their paper. The authors confirm that they give permission, or have obtained permission from the copyright holder of this paper, for the publication and distribution of this paper as part of the ICAS proceedings or as individual off-prints from the proceedings.

## References

- [1] Hasan N, Sarker P and Zaman K. Multidisciplinary robust and reliability-based design optimization of injection molding system. International Journal on Interactive Design and Manufacturing, Vol.17, pp 2957–2975, 2022.
- [2] Balesdent M, Brevault L, Valderrama-Zapata JL and Urbano A. All-At-Once formulation integrating pseudospectral optimal control for launch vehicle design and uncertainty quantification. Acta Astronautica, Vol. 200, pp 462–477, 2022.
- [3] Brevault L, Balesdent M, Bérend N and Riche RL. Decoupled Multidisciplinary Design Optimization Formulation for Interdisciplinary Coupling Satisfaction Under Uncertainty. AIAA Journal Vol, 54, pp 186-205, 2016.
- [4] Corrado G, Ntourmas G, Sferza M, Traiforos N, Arteiro A, Brown L, Chronopoulos D, Daoud F, Glock F, Ninic J, Ozcan E, Reinoso J, Schuhmacher G and Turner T. Recent progress, challenges and outlook for multidisciplinary structural optimization of aircraft and aerial vehicles. Progress in Aerospace Sciences, Vol. 135, pp 100861, 2022.

- [5] Werner Y, Vietor T, Weinert M and Erber T, Multidisciplinary design optimization of a generic b-pillar under package and design constraints, Eng. Optim, Vol. 53, No.11, pp 1884–1901, 2021.
- [6] Fang H, Gong CL, Su H, Li CN and Ronch AD. A gradient-based uncertainty optimization framework utilizing dimensional adaptive polynomial chaos expansion. Structural and Multidisciplinary Optimization. Vol. 59, pp 1199–1219, 2019.
- [7] Fang H, Gong CL, Li CN, Zhang WW and Ronch AD. A sequential optimization framework for simultaneous design variables optimization and probability uncertainty allocation. Structural and Multidisciplinary Optimization. Vol. 63, pp 1307–1325, 2021.
- [8] Giassi A, Bennis F, Maisonneuve JJ. Multidisciplinary design optimization and robust design approaches applied to concurrent design. Structural and Multidisciplinary Optimization. Vol. 28, pp 356-371, 2004.
- [9] Liu Z, Song ZZ and Zhu P. A novel polynomial chaos expansion-based method for feedback-coupled multidisciplinary design optimization under metamodel uncertainty. Structural and Multidisciplinary Optimization. Vol. 65, pp 117, 2022.
- [10]Ghosh S and Mavris DN. Methodology for Probabilistic Analysis of Distributed Multidisciplinary Architecture. Journal of Aircraft. Vol. 58, pp 536-548, 2021.
- [11]Meng DB, Yang SY, Abílio MPJ and Zhu SP. A novel Kriging-model-assisted reliability-based multidisciplinary design optimization strategy and its application in the offshore wind turbine tower. Renewable Energy. Vol. 203, pp 407-420, 2023.
- [12]Wauters J. ERGO: A new robust design optimization technique combining multi-objective Bayesian optimization with analytical uncertainty quantification. Journal of Mechanical Design. Vol. 144, 031702, 2022.
- [13]Li W, Gao L, Garg A, Xiao M. Multidisciplinary robust design optimization considering parameter and metamodeling uncertainties. Engineering with Computers. Vol. 38, pp 191-208, 2022.
- [14]Wang P, Zhu H, Tian H, Cai G. Analytic target cascading with fuzzy uncertainties based on global sensitivity analysis for overall design of launch vehicle powered by hybrid rocket motor. Aerospace Science and Technology. Vol. 114, pp 106680, 2021.